


Techno-Economic Impact of Filterless Data Plane and Agile Control Plane in the 5G Optical Metro

Pablo Pavon-Marino , Francisco-Javier Moreno-Muro , Miquel Garrich , Marco Quagliotti ,
Emilio Riccardi , Albert Rafel, and Andrew Lord

Abstract—Optical metro networks evolution driven by 5G requirements face enormous challenges. Network functions virtualized in the data centers spread to the metro nodes, IP, and optical technologies must cooperate to meet the metro traffic aggregation role. Multiple technological options exist, and carriers confront the need to economically assess them, benchmarked in realistic deployments. This paper gives relevant insights to this aim. We first construct a set of metro network benchmarks. A strategic and distinctive effort is made to incorporate metro WDM topologies, traffic profiles and daily variation patterns, fault-tolerance requisites, and network operational choices, that faithfully reflect the expected 5G metro progression for a national carrier. Then, we use these networks to assess two technological choices. On one hand, the cost-effectiveness limits in terms of CAPEX reductions and energy efficiency brought from the possibility of having an agile control plane in the metro, capable of on-demand instantiation of IT and network resources. On the other hand, we investigate the benefits of replacing ROADMs by more cost-effective filterless technologies, but just limiting this replacement to degree-1 and degree-2 optical nodes, that are prevalent (e.g. >50%) in regional metro topologies. A novel capacity planning algorithm has been developed for IT, IP and optical resources allocation and dimensioning, providing fault-tolerant designs for the realistic scenarios defined. Simulation results have been obtained using the Net2Plan NIW (NFV over IP over WDM) open-source framework. Developed algorithms and part of the testing scenarios are available for inspection in public repositories of the EU METRO-HAUL project, the umbrella for our work. Our results show CAPEX benefits in the order of 10% and energy savings in the order of 20–30% stemming from the on-demand resource allocation in the metro. In addition, degree 1 and degree 2 optical nodes have shown to be a sweet spot for applying filterless switching, with mitigated impact of the associated spectrum waste.

Index Terms—5G optical metro, agile control plane, filterless switching, techno-economic analysis.

I. INTRODUCTION

THE continued growth in demand for data, both for consumers and business, is likely to receive a further boost as 5G applications come on-stream. Exponential growth percentages in double digits lead to network capacity doubling every few years and this requires ongoing transport technology innovation to continue to provide future services. However, with the advent of 5G, this situation becomes more complex due to the differing application requirements.

The network diagram in Fig. 1 separates three transport regions of interest, encompassing access, metro and core. It also shows the node types that interface the transport regions – specifically the access metro edge node (AMEN) and the metro core edge node (MCEN). Access transport is generally evolving towards passive optical network (PON) solutions, which have a roadmap providing bandwidth growth for many years. Core transport seeks to solve a different problem, in which highly aggregated traffic is transported in fat pipes to core nodes that interface to large data centers (DCs).

This paper focuses on the optical metro segment, namely the metro transport region and the access and core-facing edge nodes, an active area of industrial and research interest. In fact, the metro network segment is getting attention due to 5G performance-aware applications, with attributes often referred to as key performance indicators (KPIs) that present requirements involving bandwidth, latency, reliability and numbers of end users (for IoT applications). These upcoming applications will require an integrated transport + IT solution including storage/compute functions based on network function virtualization (NFV).

Thus, the future optical metro network has multiple responsibilities beyond classical backhauling of traffic. Essentially, it should be able to provision and allocate distinct network + IT resources dynamically, including the assignment of storage and compute at the AMEN / MCEN together with wavelength division multiplexing (WDM) transport. Immediately it is appreciated that this new distributed data center-like architecture comes with a great deal of flexibility in how it is built and how 5G applications optimally make use of it. In this regard, it is of paramount importance to address the following questions. To what extent the metro architecture, as described in Fig. 1, is

Manuscript received November 21, 2019; revised February 1, 2020 and March 8, 2020; accepted March 12, 2020. Date of publication March 19, 2020; date of current version July 23, 2020. This work was supported in part by the European Commission for the METRO-HAUL Project under Grant Agreement 761727, in part by INSPIRING-SNI Project under Grant Agreement 750611, in part by the Spanish Government (MINECO/AEI/FEDER, UE): ONOFRE-2 Project under Grant TEC2017-84423-C3-2-P, and in part by the Go2Edge Project under Grant RED2018-102585-T. (Corresponding author: Miquel Garrich.)

Pablo Pavon-Marino is with the Universidad Politécnic de Cartagena 30202, Cartagena, Spain, and also with the E-lighthouse Network Solutions, 30202 Cartagena, Spain (e-mail: pablo.pavon@upct.es).

Francisco-Javier Moreno-Muro and Miquel Garrich are with the Universidad Politécnic de Cartagena, 30202 Cartagena, Spain (e-mail: javier.moreno@upct.es; miquel.garrich@upct.es).

Marco Quagliotti and Emilio Riccardi are with the Technology Innovation of Telecom Italia, 10148 Torino, Italy (e-mail: marco.quagliotti@telecomitalia.it; emilio.riccardi@telecomitalia.it).

Albert Rafel and Andrew Lord are with the British Telecom, Ipswich IP5 3RE, U.K. (e-mail: albert.2.rafel@bt.com; andrew.lord@bt.com).

Color versions of one or more of the figures in this article are available online at <http://ieeexplore.ieee.org>.

Digital Object Identifier 10.1109/JLT.2020.2982131

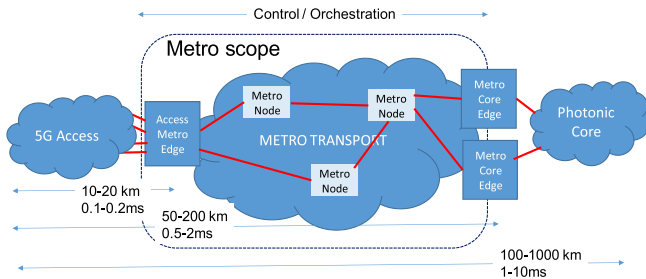


Fig. 1. Schematic of end-to-end network.

required to deliver the 5G applications on the horizon? How can this architecture be built in a cost-effective way?

These two questions have been addressed within the EU METRO-HAUL project [1]. In this paper, a strategic effort is placed in building a benchmark of realistic metro scenarios in terms of topology, traffic, resilience requisites, and practical operational choices, that fairly reflect the challenges that 5G poses in the metro, and the options for handling them. A part of the input data and the totality of the simulation software and algorithms for this benchmark are open-sourced and publicly contributed to the community, through the open-source Java-based Net2Plan network planning tool [2]. We concentrate in assessing two technological choices. First, the cost savings achievable from having a dynamic and agile control plane capable of on-demand provisioning network and IT resources when faced with expected daily traffic variations. Second, we benchmark filterless optical architectures, as a cost-effective alternative to reconfigurable optical add-drop multiplexer (ROADMs), but just restricting their use to degree-1 and degree-2 metro nodes. This has been identified as a sweet-spot utilization, where the spectrum waste introduced by filterless nodes is mitigated, while the cost benefits are multiplied by the economies of scale.

The remainder of the paper is structured as follows: Section II describes the related work regarding techno-economic studies in the scope of 5G-aware optical networks. Section III presents the definition of the reference scenario assumed in this work. The targets of the study are exposed in Section IV. A capacity planning algorithm is presented in Section V, the basis for the network dimensioning. Next, the simulation set up and the numerical results obtained are shown in section VI. Finally, section VII draws up the main conclusions of this paper.

II. RELATED WORK

In general terms, techno-economic studies aim at assessing the impact of a technological solution considering both its technical and economic performances. These studies are conducted in all network segments, for different technological choices and cost-performance trade-offs, and optical networks are no exception. Illustrative examples include, routing solutions for energy efficiency [3], restoration and protection mechanisms considering network cost minimization [4], [5], client-to-line node architectures combined with transmission techniques for cost-effective network dimensioning [6], [7], multi-layer architectures and

approaches for capital expenditures (CAPEX) reduction [8]–[10], transmission technologies to reduce transponders count [11] and Raman amplification technology to reduce amplifiers count [12] just to mention a few. Here, we overview techno-economic works concentrating on the three areas covered in our study: the impact of 5G in metro optical networks, comparisons between filterless and ROADM (i.e. filtered) node architectures, and agile versus static control-plane mechanisms. Subsequently, we highlight our contribution compared to related work.

A. 5G Impact in Metropolitan Optical Networks

The accomplishment of the 5G KPIs [13] entails profound technological implications in the overall telecommunications infrastructure. Although 5G is to some extent a mobile-oriented technology, network (re)evolution is occurring in the access segment and the metro-core segment.

On the one hand, many recent works concentrate in assessing the effects of 5G deployment in access networks from techno-economical perspectives. For instance, the drawbacks in radio interference and resource management (RIRM) in 5G radio access networks (RANs) are covered in [14], whereas [15] considers multi-layer protection and restoration schemes for a CAPEX evaluation in terms of power consumption and network capacity, in the view of cloud RAN (C-RAN) 5G networks.

On the other hand, the studies [16] and [17] focus on the implications of 5G in the metro-core part of the network. In [16], authors exhaustively analyze the possible challenges in 5G backhaul metro networks. A cost evaluation of the content distribution in multiple data centers considered for the 5G core mobile network with SDN and NFV capabilities is addressed in [17]. Techno-economic aspects of the processing costs associated with virtualized network functions (VNFs) in service chains is addressed in [18]. Optical metro-area networks are considered in [19], which presents an algorithm for dynamic service-chaining allocation that jointly minimizes the average number of nodes required to host VNF instances as well as the blocking probability, which in turn reduces operational expenditures. In more detail, [19] considers the end-to-end latency contributions of both VNF deployment and routing in the optical network (i.e. a 5G KPI requirement).

B. Filterless Versus Filtered Nodes

Techno-economic studies commonly leverage advances in technology to explore cost reductions, and the ordinary trend is to rely on the usage of more spectrum efficient technologies to attain economic benefits. For instance, advances in electrical switching [6], flexible transmission [7] or purely optical-layer techniques [11] commonly target transponder count reduction; or advanced amplification to reduce amplifier count [12]. However, a recent approach has emerged exploring the opposite direction: to diminish the technological efficiency in the pursue of an aggressive cost reduction. Such approach is based on filterless optical node architectures that employ cheap couplers/splitters instead of expensive reconfigurable wavelength-selective filters (see Section IV.A). At the expense of a reduction in the spectral efficiency performance, filterless solutions hold the

promise to provide enormous CAPEX reduction. [20] can be considered one of the first works to explore filterless nodes, in which authors evaluate the trade-off between the cost benefits and the performance losses due to lower signal-to-noise ratios. Furthermore, in [21], filterless architectures are evaluated as a solution to be applied in optical white-boxes based on optical coupler/combiner devices. The cost-effectiveness of different transmission techniques is covered in [22] while considering the maximum network throughput which can be achieved in filterless optical networks according to different spectrum management policies. The work in [22] reinforces the economical convenience of market-ready semi-elastic transmission techniques against non-commercial hitless full-elastic solutions in filterless networks.

C. Agile Versus Static Mechanisms

Intelligent and optimization mechanisms in the control plane that in turn better exploit the resources of the data plane are fundamental to the accomplishment of the 5G KPIs [13]. There are several works that explore how an agile control plane can benefit to save optical resources when dimensioning the optical network, when the daily or weekly traffic variations can be estimated [23], [24]. However, to the best of our knowledge, no works contemplate the daily traffic profile as a basis for advanced control-plane actions impacting on the data plane to reduce economic costs in *both* the network and IT infrastructure. Most of the related work simply provides the technological solutions in terms of architectures or protocols. Clear examples are [25], in which authors propose a novel technique to orchestrate mobile access networks by exploiting the benefits of the SDN and NFV paradigms. As a follow-up of this last work, in [26] authors upgrade the control, management and orchestration operations into a unified agile control plane. This proposal considers multi-layer optical networks to cope with the challenges regarding the 5G deployment.

D. Our Contribution

The contribution contained herein is based on seminal works that comprise: i) consistent and realistic 5G metro network simulation frameworks [27], ii) NFV-over-IP-over-WDM multi-layer network modelling [28], iii) optical node comparison in terms of cost-performance trade-off analysis [29], [30], and iv) SDN/NFV-based agile control plane integration and evaluation for access and metropolitan optical networks [31], [32]. Additionally, to allow repeatability and accessibility, our developments are coded with open-source tools and are available in METRO-HAUL repositories [33].

The state-of-the-art research analyzed in this section presented solid contributions to the literature in network economics. However, we believe our paper fills several relevant gaps. First, the detailed benchmark scenarios presented are themselves a significant contribution, stemming from a carrier view, that could help to drive future studies in the 5G metro evolution. The capacity planning algorithm described, used to dimension and allocate the IT resources, the IP resources, and the optical resources, considering requisites coming from fault-tolerance

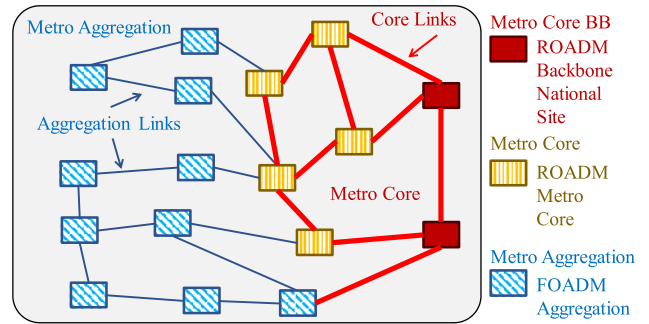


Fig. 2. Topology structure of Telecom Italia regional networks.

and realistic practical operation decisions, is novel. The agile vs. static and filterless vs. ROADM interrogations have not been addressed before in this context, and give significant insights for future deployments.

III. REFERENCE SCENARIO

This section describes several network aspects that make up the reference scenario: the topologies, traffic assumptions, fault tolerance requisites, and other operational choices considered.

A. Telecom Italia Reference Fiber Topologies

The set of reference networks used in the study are inspired mainly by the current Telecom Italia metro regional WDM transport network serving about 1,500 central offices in Italy due to its topological complexity and heterogeneity that well exemplifies the categories of metropolitan networks of interest in the present work. This WDM network is widespread all over the country, is in continuous evolution and is gradually replacing other technologies like dark fiber, point to point WDM or packet transport in remote rural areas.

The metro-regional infrastructure is composed of 14 separated metro-regional networks (some including more than one administrative Italian region, which are 21 in total). As shown in Fig. 2 each metro-regional network is structured into two tiers: a meshed core and an aggregation part connected to the core by means of rings or weakly meshed topologies. Each regional network is a transparent island including the core and the aggregation, i.e. any node can be reached in optical transparency by any other node within each regional network. Optical transparency is not supported between regional networks and from regional networks to the National backbone. At present, each core node is usually equipped with a ROADM with up to eight express degrees, while aggregation nodes are equipped with FOADMs (Fixed OADMs, hard-wired versions of ROADMs, that require on-site manual manipulations for configuring them) with up to four express degrees. Let us clarify that express degrees interconnect input and output ports to provide connectivity from/toward other ROADMs in the network, whereas add/drop degrees provide the required connectivity between the express degrees and the transmitters (receivers) for lightpaths with source (destination) at the local node [34]. Network diameters range from about 200 to 500 kilometers but,

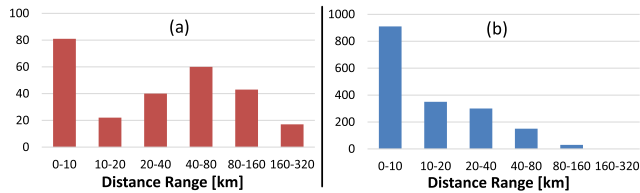


Fig. 3. Distribution of link lengths in Telecom Italia metro-regional networks. (a) Core part, (b) aggregation part. (10-20 means $10 < D \leq 20$).

due to the logical topology of the higher layer (e.g., L2/L3), no optical lightpaths are commonly required between distant nodes. The evolution and future structure of this metro-regional network is a subject of intense study by the planning department in view of the forthcoming 5G widespread deployment. Results achieved in this work are expected to give useful indications for this development.

Concerning the fiber, G.652 (SMF) is highly predominant. Link lengths are very scattered, ranging from hundreds of meters to hundreds of kilometers. Only a few long links require optical line amplifiers. Diagrams of Fig. 3 report the distribution of link lengths on both the core and aggregation parts of the network, averaging the values at the national level. Two most significant fractions of core links (Fig. 3(a)) are in the range of 0–10 km and 40–80 km. This is because the connections between core nodes within a metropolitan area fall in the first class, while the second class accounts for the typical inter-city distances within each metro-regional domain. Aggregation links (Fig. 3(b)) are commonly very short (in the range 0–10 km). The low number of long links (greater than 40 km) corresponds to connections between nearest nodes in sparsely inhabited areas. Concerning the topological degree of the network, the fiber connectivity of the aggregation part shows a degree from 2 to 4, with the average value around 2.5, while the connectivity of metro-core nodes is between 4 and 8 with an average of 5.5.

The Telecom Italia metro-regional topologies are used as a realistic framework to perform the planning studies presented in this work. More specifically, the reference networks are used both to design the WDM network on the fiber topology, and for assigning the central office role: (i) nodes in the metro core are assigned the role of MCEN in the METRO-HAUL architecture, and (ii) MCEN-BB (MCEN-backbone) if the metro node is connected to the core. Alternatively, (iii) aggregation nodes take the role of AMEN in the METRO-HAUL architecture. Additionally, core nodes also have traffic aggregation functions, for serving the users situated nearby. As such, in this paper we will use AMEN to refer to both the aggregation nodes, as well as the aggregation functions in MCEN and MCEN-BBs.

As the 14 metro-regional WDM networks are rather different from each other in terms of number of nodes, extension of area covered and population served, a selection of two representative cases have been chosen for techno-economic analysis. These two networks are representative because they exhibit the same characteristics of the entire composition of all Telecom Italia regional networks. In addition, a Dense Urban metro network is also selected as a part of a wider regional network of about 200

TABLE I
TOPOLOGICAL DATA OF SELECTED REFERENCE NETWORKS

| Network | Nodes (deg 1-2) | Core nodes | Tot. links | Core links | Area [km ²] | Pop. |
|-------------|-----------------|------------|------------|------------|-------------------------|------|
| Reg. Small | 52 (30) | 6 | 72 | 10 | 18k | 2.5M |
| Reg. Normal | 102 (59) | 11 | 143 | 19 | 28k | 4.5M |
| Dense Urb. | 36 (8) | 28 | 54 | 42 | 200k | 1.5M |

nodes in total to allow a case study focused on a metro network covering exclusively a big dense urban environment.

In Table I the main characteristics of the selected reference topologies in terms of nodes, links, area covered and population served are reported. Note that for Regional networks (small size, and normal size cases) the number of core nodes is a small fraction of the total number of nodes (in the order of 10%), and the number of degree 1 and 2 nodes is above 50%, while in the Dense Urban the core nodes are the majority. Among the core nodes, few of them are connected to the National backbone. Specifically, two core nodes are connected with the National backbone for all the networks listed in Table I.

B. Traffic Model

The traffic used for dimensioning the reference networks is generated by a traffic model, that allows the calculation of the aggregated background traffic, distinguishing between residential and business users. This is considered to be sufficient for the targeted macroscopic techno-economic analysis. More fine-grained traffic models that pursue an individual evaluation of applications coming from different vertical markets, are not considered in this work.

The traffic flows are computed in terms of data rate (b/s) in the busy hour between the users connected to the access and the service points which can be located within the metro scope or outside it (in the last case they are reached through the backbone). Both directions, the downlink component (stream from the network to the user) and the uplink component (from the user to the network), are considered. For each traffic type defined, the downlink (DL) component is explicitly calculated, while the uplink (UL) component is derived as a percentage of the downlink. Only the data plane traffic is considered, the most relevant in terms of volume, and with the most significant impact on the metro architecture and dimensioning.

The 5G System architecture [35] is taken as a framework for the traffic model used in this paper (Fig. 4). The Data Plane, shown in the lower part of Fig. 4, is modeled by the chain of user equipment (UE), the access network (AN), which can be the 5G RAN, the user plane function (UPF) and the data network (DN). The UPF plays the central role in routing the traffic to desired application and network functions. In 5G architecture the UPF is not a single functionality for all traffic but can be specialized per service or traffic type. DN represents an external entity to the 5G system, located inside or at the border of the metro network, which offers data plane connectivity (including connectivity with the operator backbone or to the Internet) or even other network service; in general, it can be seen as a network service platform. The metro network is responsible for

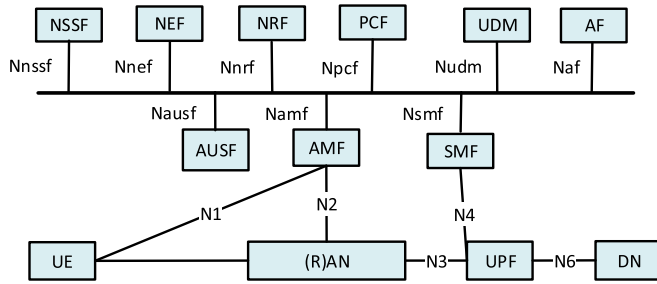


Fig. 4. 5G System architecture interface representation (top: control plane, bottom: user plane). (radio) access network ((R)AN), access and mobility management function (AMF), application function (AF), authentication server function (AUSF), data network (DN), network exposure function (NEF), network slice Selection function (NSSF), NF repository function (NRF), policy control function (PCF), session management function (SMF), unified data management (UDM), user equipment (UE), user plane function (UPF); Nxxx are service-based interfaces and N# are reference points. Source: 3GPP-TS-23.501 [36].

transporting the traffic between the (R)AN and the DN, covering both the segment between the (R)AN and UPF and the one between the UPF and DN.

Different specialized UPFs can be located either closer to the access or more centralized. In the simplified model used for this work, two UPF types are considered. First, a centralized UPF is placed in each of the MCEN-BB nodes: the two MCENs connected to the Backbone (UPF of type 1, UPF1). Second, a UPF is assumed to be located near the edge, in all the AMENs and MCENs nodes (UPF of type 2, UPF2).

Three macro types of traffic are considered by the model. For each of the three macro traffic types, Fig. 5 exemplifies the network parts and user plane functions involved (UPF1 or UPF2), as well as the traffic flows generated. More specifically, the traffic types are the following ones.

- **A1 - Point-to-point traffic (P2P)** between two user terminals (fixed or wireless-mobile) and which is assumed to transit always on a centralized UPF (UPF1). The source of this traffic is a user served by an AMEN node, and the destination can be at another metro node belonging to the same metro network (green flows in Fig. 5(a)), or another point outside the metro network reached through the interconnection gateway to the backbone (grey flows in Fig. 5(a)). In our case, the gateway used will be the closest MCEN BB node, according to the optical latency.
- **A2 - Heterogeneous server-mediated traffic**, which involves a user terminal connected to an AMEN node and a server located in a centralized metro node (an MCEN interconnected with the backbone, i.e., an MCEN BB, red flow in Fig. 5(b)) or in a server outside the metro (grey flow in Fig. 5(b)). As for A1, this traffic subtype also transits through a centralized UPF (UPF1). Also, the MCEN-BB node used will be the closest one in optical latency.
- **A3 - Edge computing and storage services**, which include caching services for popular contents, edge computing and low latency new 5G services. The location of the enabling DCs can be extremely decentralized in the AMEN where the user is connected (grey flow in Fig. 5(c)), or it can be

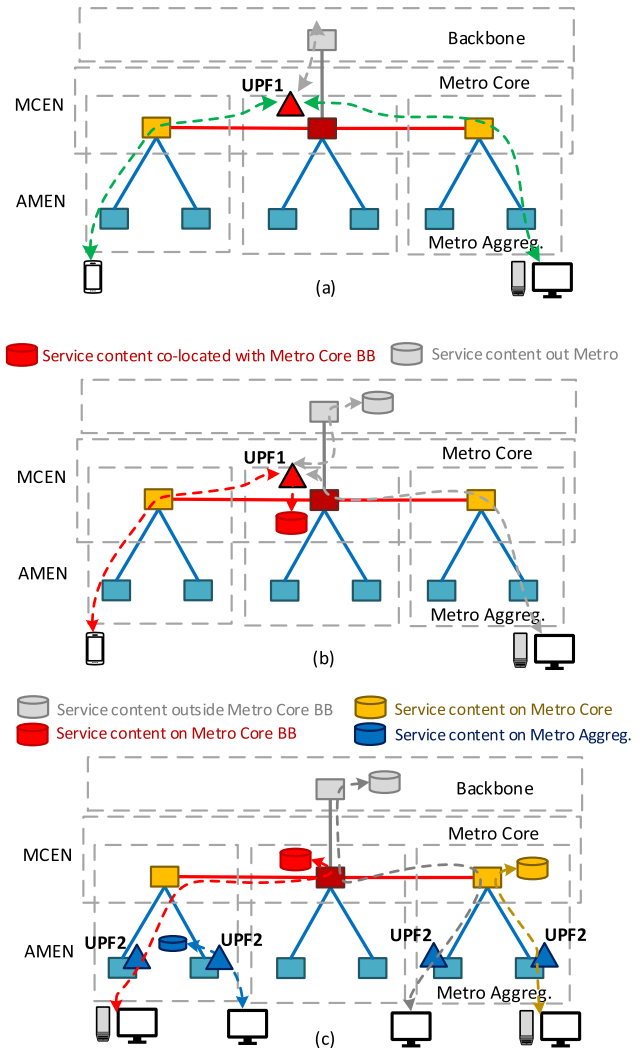


Fig. 5. Scheme of traffic flows for the three traffic types, a) point-to-point traffic (A1), b) heterogeneous server-mediated traffic (A2), c) edge computing and storage services (A3).

placed in an intermediate point (in the closest MCEN to the user measured in km, yellow flow in Fig. 5(c)) or in an even more centralized point next to the backbone (the closest MCEN BB node in optical latency, red flow in Fig. 5(c)). This traffic type relies necessarily on the UPF located on the edge (UPF2) because the content can be downloaded or the service delivered from the DC located at the AMEN where the user accesses the network.

The traffic model used to generate the traffic flows in the network for the scenarios analyzed is based on the traffic generated by each node, which is then used to calculate the traffic flows applying the modeling and the associated parameter values of traffic types described above. Only a high level description of the traffic generation used for the study cases presented in this article is given hereafter; the reader can find the complete model in [36].

The starting point for calculating the traffic generated by a node is the collection of its attributes, which are the number of

TABLE II
NODE INDEPENDENT TRAFFIC PARAMETERS ASSOCIATED TO THE ACCESS

| Parameter | Term: | Short | Med. | Long |
|--|-------|-------|-------|------|
| Residential fixed line per household | | 0.5 | 0.52 | 0.55 |
| Business fixed line per household | | 0.05 | 0.055 | 0.06 |
| Average DL traffic per residential line [Mb/s] | | 1.8 | 3.7 | 7.6 |
| Average DL traffic per business line [Mb/s] | | 3.6 | 7.4 | 15.1 |
| DL Traffic per 4G site at busy period [Mb/s] | | 100 | 140 | 200 |
| DL Traffic per 5G RRU at busy period [Mb/s] | | 500 | 800 | 1000 |

TABLE III
PARAMETERS USED FOR TRAFFIC FLOW CALCULATIONS

| Parameter | Traffic type | | |
|--|--------------|-----|-----|
| | A1 | A2 | A3 |
| Share of the total AMEN downlink traffic | 10% | 30% | 60% |
| % of uplink traffic wrt downlink traffic | 100% | 30% | 10% |
| % of traffic going outside the metro area | 33% | 80% | 25% |
| % of traffic exchanged locally in the AMEN | - | - | 25% |
| % of traffic exchanged with the nearest MCEN | - | - | 25% |
| % of traffic exch. with the nearest MCEN-BB | 67% | 20% | 25% |

households and the number of 4G and 5G radio sites gathered. As the study is conceived as a multi period analysis focused on three timeframes (short, medium and long term), those node attribute values change accordingly (in particular, 5G radio sites gathered by a node increase significantly with time while others remain quite stable).

Combining the node attributes with other independent parameters like fixed line market penetration for both residential and business (expressed as lines per household), average DL traffic per residential fixed line and per business fixed line, and downlink traffic per 4G and per new radio (NR)-5G radio site, it is possible to calculate the four contributions (fixed residential, fixed business, 4G radio and NR-5G) to the downlink traffic generated by the node. Values of the above parameters used in this study are reported in Table II. Traffic is always referred to the busy period of the day. Please note that also these node independent parameters change with the period of the analysis and, in particular, they increase their values according to the uninterrupted Internet growth and due to the development of new traffic greedy services. More details can be found in [36].

Once the total downlink traffic generated by a node has been calculated, the contribution of the three traffic types (A1, A2, A3) and their subflows as shown in Fig. 5, is governed by fixed percentages, as shown in Table III. The first row in the table indicates the weight of each traffic in the total. The second row reports uplink traffic, as a percentage with respect to the downlink traffic in each service type. For instance, as A1 traffic is symmetrical, this percentage is 100%. In contrast, the cacheable traffic, which is highly asymmetrical (services delivering contents like video streams to the residential user involve the data transmission largely in downlink direction), has an uplink traffic of only 10 % of the downlink. Rows from three to six include each of the shares of total node traffic exchanged with the four significant points in the metro architecture.

Applying the above model to the three reference networks of Table I and taking into account the parameters of each time period, the figures of average downstream traffic per node

TABLE IV
AVERAGE TRAFFIC PER NODE FOR THE FOUR REFERENCE NETWORKS

| Network | Downstream traffic per node [Gb/s] | | |
|-------------|------------------------------------|-------------|-----------|
| | Short term | Medium term | Long term |
| Reg. Small | 20.2 | 49.1 | 112.3 |
| Reg. Normal | 23.9 | 58.0 | 133.1 |
| Dense Urban | 21.2 | 60.0 | 146.1 |

TABLE V
DOWNSTREAM TRAFFIC DETAIL (DENSE URBAN TOPOLOGY)

| Traffic contribution | Short term | Medium term | Long term |
|----------------------|------------|-------------|-----------|
| Fixed Residential | 78% | 59% | 53% |
| Fixed Business | 16% | 12% | 11% |
| Radio 4G | 6% | 3% | 2% |
| NR-5G | 0% | 26% | 34% |

reported in Table IV have been obtained. Please note that the traffic per node are values averaged over all the nodes and some variability exists among them, both in the traffic and in the shares of traffic generated by each of the four contributions (fixed residential, fixed business, 4G radio and NR-5G). Nevertheless, the variance of overall traffic gathered by each node is relatively small. This is because the geographic distribution of the nodes is such that each node collects traffic from approximately the same number of customers. With the parameters setting used, the upstream traffic results in an average in the order of 25% of the downstream. For the same reason the average traffic per node is very similar among the three networks in short and medium term, while for the long term the expected higher penetration rate of 5G service in dense urban areas causes the greater value of traffic per node for the Dense Urban network.

To illustrate the contribution of fixed and mobile access to the total traffic in the three periods, Table V displays the case for the dense urban reference network. The value of 0% of share of NR-5G in the short term is due to the existence of a very limited number of NR-5G plants and terminals in the early deployments of 5G. In this phase 5G services rely mainly on 4G for radio access and its traffic is not yet significant in terms of volume compared to other components. Then overall traffic evolves from the predominance of the fixed line contribution in the short term, to a significant share due to NR-5G in the long term.

C. Multi-Hour Traffic Profile

It is well known that in the metro networks traffic exhibits significant fluctuations along the day, a phenomenon studied on multiple occasions [22], that comes from natural human activity patterns. The so-called multi-hour traffic profile of each service is an attempt to represent how the service intensity varies along the day, typically in per-hour batches. Such variations can have profound implications in resource allocation, if the network is agile enough to assign resources on-demand instead of being dimensioned for the worst-case traffic.

To study this possibility, we consider in this paper that the residential services and the business services, follow the traffic fluctuation profile shown in Fig. 6, which has been presented in METRO-HAUL project as a realistic traffic profile observed in metro networks [36]. Note that Fig. 6 shows a normalized time

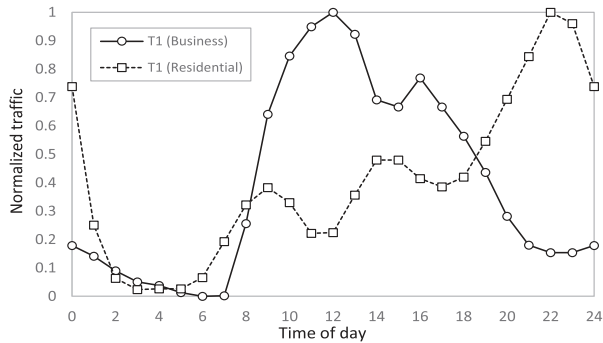


Fig. 6. Normalized traffic weight variation along the day [36].

variation of the intensity, with respect to the traffic observed in the peak hour in each node for each residential and business profiles, which will shape the traffic of every node. In addition, it is worth to mention that while the business traffic has its peak intensity in the morning, the residential traffic peaks in the evening, driven by the video-on-demand services.

D. IP Over WDM Operational Choices

According to the METRO-HAUL view, we assume that each of the A1, A2, A3 services offered in the network are structured in *network services*, following the ETSI MANO naming convention, that in this paper take the form of service chains: a sequence of *physical* or *virtualized* network functions (NFs) interconnected via *virtualized links*. Network functions deployed are the user traffic aggregation function, the UPF2, edge and caching services in each AMEN, and the centralized UPF1s in each MCEN-BB. The virtualized links correspond to the subflows shown in Fig. 5 that carry the service traffic between the NFs.

In this paper, we consider that each virtualized link is realized as an IP circuit between the two end NFs, that carries the traffic between them. Virtual links between NFs in different metro nodes are accomplished via IP end-to-end connections across the metro network, where the sequence of IP links to be traversed can be individually determined. This can be performed today with conventional IP technologies like MPLS-TE, or with more evolved SDN-based approaches.

The IP over WDM operation is based on link aggregation groups (LAG) [37], a common operational choice in metro and core networks. In particular, at most one IP link exists between two metro nodes, implemented as a LAG grouping together, and aggregating the capacity of all the lightpaths between the LAG end nodes. The IP traffic through a LAG is spread among its lightpaths. This is typically executed via hash-based hardware mechanisms like those in [37], that forward through the same lightpath the IP datagrams of the same connection. Thanks to this, order is preserved among same TCP connection packets, and thus TCP-performance degradation is avoided, even when aggregated lightpaths follow different optical paths. Since hash-based mechanisms operating at wire-speed are challenging, they typically require all the LAG members to be of the same line rate. This technological constraint is also considered in this paper.

E. Fault-Tolerance Design Requirements

Fault tolerance is a requisite in carrier networks, and cannot be sidestepped in any techno-economic study. In our reference networks, we consider two fault tolerance requirements to be satisfied:

- Tolerance to single failure of a WDM duct, that contains all the WDM links between two nodes, in both directions. This tolerance target is not required in a limited number of cases, corresponding to access nodes in leafs of the WDM topology, this means, connected to the rest of the network by a single WDM duct, with no alternative path in the WDM topology.
- Tolerance to single failure of an MCEN-BB node, which is considered a critical structure with a large impact in case of malfunction. The fault tolerance requirement means that if a MCEN-BB fails, the network resources should be enough to fully carry the traffic from/to each node through the next closest MCEN-BB.

IV. TECHNO-ECONOMIC STUDY TARGETS

The techno-economic study presented in this paper is aimed at evaluating the cost vs. performance trade-offs related to two technological choices:

- *Optical data plane*: We compare an optical metro fully equipped with non-blocking ROADMs in the data plane, with a network where more cost-effective filterless nodes are used, just in degree-1 or degree-2 AMEN nodes, appearing in leaf and ring segments of the optical metro topology, being the rest of the nodes regular ROADMs.
- *Agile control plane*: Agile control plane enabling *dynamic* allocation of IT, IP and WDM network resources, adapting to a varying demand.

A. Filterless vs. ROADM Optical Switching Architectures

Filterless optical switching architectures have been presented and analyzed in seminal works like [20] or [21]. The idea behind its philosophy, is removing expensive optical filtering capabilities in the express degrees of ROADMs, to have a more cost-effective solution, at the expense of wasting spectrum. Let us recall that express degrees are devoted to the transparent optical routing from/to other sites whereas add/drop degrees refer to the source/termination of lightpaths [34].

The filterless nodes considered have a drop & waste (D&W) switching architecture as shown in Fig. 7(a). In D&W nodes, the dropped signals are not filtered out, but instead propagate occupying spectrum in the outgoing direction after the drop, until a regular ROADM node is reached that blocks the signal.

The spectrum waste downside is illustrated in Fig. 7(b), which corresponds to a well-known horseshoe topology: a line of D&W filterless nodes of degree two, ended in two regular ROADMs. Fig. 7(b) helps to understand the performance loss caused by the waste operation. Lightpath LP1 from node D to E in wavelength λ_1 has no waste, since it is dropped in a ROADM. Still, the λ_1 spectrum not wasted in fibers from A to D *cannot anyhow be used* by any lightpath. Actually, the lightpath LP2 from A to B,

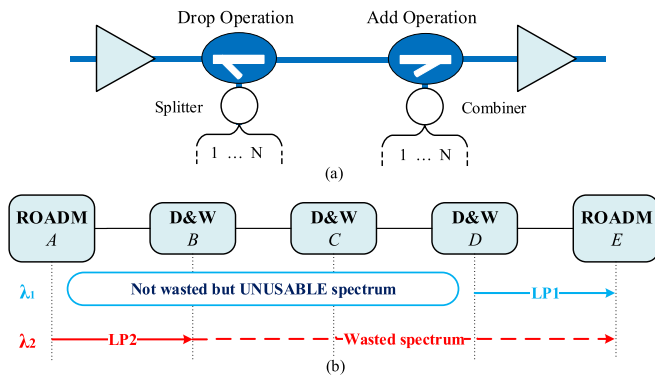


Fig. 7. a) D&W Filterless design and b) propagation example in a D&W Filterless node operation. D&W: drop and waste; ROADM: reconfigurable optical add-drop multiplexer.

assigned to λ_2 in the figure, could not be assigned to λ_1 since its waste would destroy LP1 signal.

From a network-wide perspective, the waste operation can lead to the appearance of *lasing loops*, i.e. cycles of fibers and filterless nodes, that result in continuous propagation of waste signals. Lasing loops need to be prevented since they compromise the entire network performance. In this regard, our work in [38] presents a specific extension of Net2Plan [2] for filterless-aware offline planning and analysis. In particular, [38] analyzes the spectrum occupation of the lightpaths, warning about clashes and/or internal blocking events, considering the propagation of the legitimate and waste signals in the fiber, among other relevant optical-layer aspects (e.g. WDM line engineering) and network consideration (e.g. cost & energy consumption).

B. Agile Control Plane: Static vs. Dynamic Planning

The IP-level user traffic demand follows a multi-hour pattern as described in Section III.C, where business traffic and residential traffic intensities change during the day, but according to different daily patterns. As can be seen in Fig. 6, business traffic peaks in the morning, while residential traffic peaks in the evening.

Since the traffic is not constant, on-demand allocation of resources is a potential source of CAPEX and operational expenses (OPEX) savings. In our case, if the network is equipped with an agile control plane, two types of on-demand allocations are possible:

- On-demand allocation of IT resources to VNFs in the nodes. This means that IT resources in a node can be *shared*, i.e. IT resources in a particular node, used in the morning for running VNFs of business traffic, can be used in the evening for placing VNFs of residential traffic. Note that this would apply to the network functions that are implemented as *virtualized* NFs. In this paper we assume that this happens for all the network functions, the clear trend in 5G evolution.
- On-demand allocation of lightpaths. Optical connections are set up and torn down on demand, and transponders in a node can be *shared*, i.e. a transponder in node A, used in

the morning for a lightpath to node B, can be used in the evening for a lightpath to node C.

In terms of planning, the existence or not of an agile control plane results in two different planning strategies:

- *Static worst-case traffic planning.* Since IT and network resources cannot be shared among different services, the network is dimensioned for the worst-case traffic. This means that *for each service chain*, we compute the highest traffic injected during the day. Then, the network is dimensioned for traffic composed of these worst-case service chains. Note that this means dimensioning the network for traffic that practically never happens, since residential service chains peak in the evening and business ones in the morning.
- *Dynamic multi-hour planning.* The network is assumed to be fully re-planned every hour. Therefore, the IP traffic shifts lead to: (i) variations in the traffic carried in the IP links, and potentially new IP links created, and unused IP links tore down, (ii) variations in the amount of traffic to process by the VNFs. To cope with IP link traffic variations, the number of lightpaths in the LAG and their optical paths are re-planned so capacity is enough, for all the failure situations for which the design is requested to be tolerant. Additionally, each VNF is assigned the required IT resources in each hour of the day. Finally, *for each node* the number of transponders of each type to be placed and the amount of IT resources, are given by the worst-case needs *during the day* in that node.

Note that the dynamic multi-hour planning described has limited operational penalties in terms of service disruption. The dynamic modification of the number of lightpaths in a LAG can be made without interfering with the IP layer routing protocols, since IP topology is unaffected and can be unaware of such modifications [37]. LAGs in carrier-grade hardware are hot-configurable, seamlessly making use of the available capacity in the LAG current members. In addition, each LAG can adjust its capacity independently of others, and by using predictive schemes, new lightpaths can be allocated *before* they are actually needed, and released *after* they are needed, with minimum probability of disruption or waste of resources. VNF resizing would benefit from similar predictive schemes, that permits assigning IT resources on-demand [39]. This can also be considered a mature technology. Automatic resizing schemes are commonplace in the cloud managers, which often permit plugging in predictive algorithms for scheduling the capacity adjustments (e.g. [39], or other examples in [40]).

V. CAPACITY PLANNING ALGORITHM

In this section, we describe the capacity planning algorithm developed to supply the necessary intelligence in the deployment of the techno-economic analysis. The objective of this algorithm is to provide a complete resource allocation solution, applied both in static and dynamic techniques. For the worst-case static option the algorithm is executed once, where the traffic of each service chain is the worst along the day for that service chain. In contrast, to emulate the behavior of dynamic multi-hour

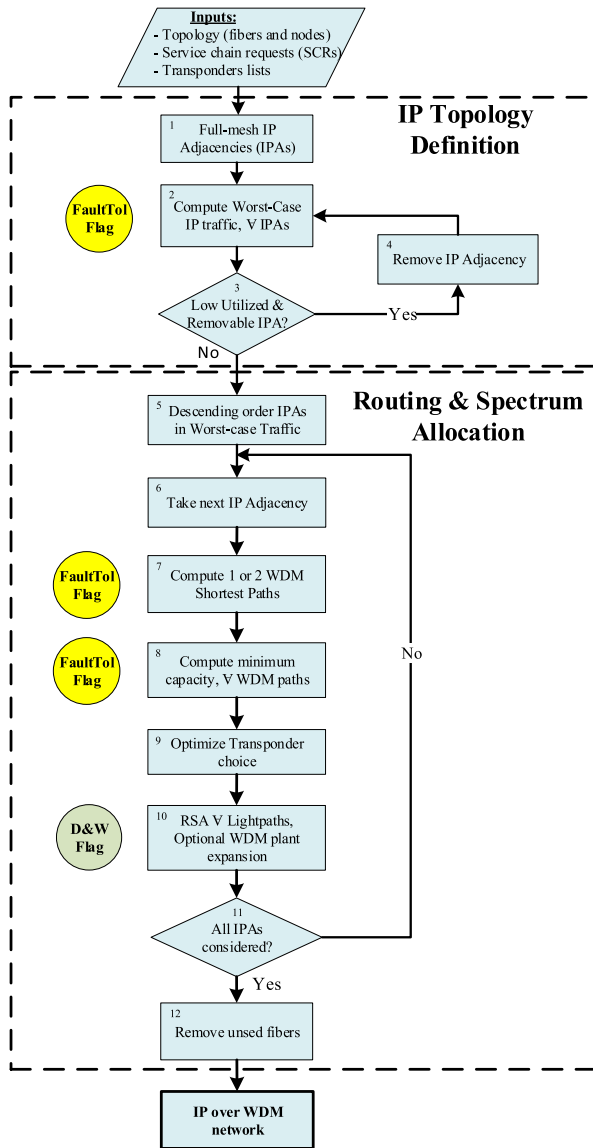


Fig. 8. Flow diagram of the capacity planning algorithm. D&W: Drop and Waste; IPA: IP adjacency; RSA: routing and spectrum allocation.

planning, the algorithm is run 24 times, one for each 1-hour network planning slot, where the service chain traffic are the ones relevant at that hour.

Fig. 8 sketches a flow diagram of the algorithm, in which its blocks are numbered and used in parenthesis in the following. The algorithm inputs are:

- The network WDM topology: the fiber and node sets. Nodes of optical degree three or more are all ROADMs, while degree one and two nodes, can be filterless D&W or ROADMs.
- The set of traffic demands represented by a set of service chain requests (SCRs), i.e. a sequence of types of physical or virtualized network functions (NFs) to traverse via virtualized links, and the amount of traffic injected in the origin of the chain.
- The list of available transponders usable for MCEN-to-MCEN connections, and the ones for those connections

involving an AMEN. Each transponder is characterized by its net line rate (Gb/s), its maximum optical reach (km), and its spectrum occupation (GHz).

The algorithm can be run with the fault-tolerant flag active, meaning that the produced design is required to satisfy the fault tolerance requisites described in Section III.E. A detailed description of algorithm steps follows.

A. IP Topology Optimization

In the first stage, (1) the algorithm computes the set of IP adjacencies (IPAs) in the network, with the prospect of implementing each one by a LAG, aggregating the lightpaths between the adjacency end nodes. Initially, an IP adjacency is placed between every two MCEN nodes, if they are within the optical reach of at least one transponder type assigned to MCEN-MCEN lightpaths. Similarly, AMEN to AMEN and AMEN to MCEN, IP adjacencies are added if a lightpath is possible between them according to, at least, one associated transponder reach.

Given a tentative IP topology, (2) we compute the worst-case amount of traffic that each IP adjacency will carry. This means, the highest value among:

- *Traffic in the non-failure state.* The traffic in each virtualized link is routed through the shortest path in number of IP hops.
- *Traffic in each MCEN-BB failure state.* Service chains headed to/from the failed MCEN-BB are reconfigured to use the next closest one. Then, the traffic in each virtualized link is routed through the shortest path in number of IP hops over the surviving IP topology.

If the design is not required to be fault tolerant, the second point above is not implemented in the worst-case traffic calculation, and thus only the non-failure state is considered.

Once the worst-case per IP adjacency traffic is obtained, (3,4) the algorithm tries to remove those IP adjacencies with too little traffic. For this, the algorithm orders them in increasing order, according to the IP traffic carried (the highest in the two directions). Then IP adjacencies are iterated one by one. For each, we compute the lower line rate possible for the lightpaths implementing that IP adjacency, according to the assignable transponders. If the IP traffic is below the 10% of such rate, and the adjacency end nodes are reachable by an alternate IP path, the IP adjacency is removed, and all the service chains are rerouted accordingly. The process continues, until no IP adjacency is eligible to be removed.

B. Routing and Spectrum Assignment (RSA) Optimization

The second phase of the algorithm creates the lightpaths realizing the IP adjacencies, solving the routing and spectrum allocation (RSA) problem for each lightpath. (5) IP adjacencies are sorted in decreasing order according to the worst-case IP traffic carried (considering MCEN-BB failure situations if fault tolerance is requested). Then, (6,11) for each IP adjacency, (7) the algorithm computes the WDM path or the WDM path pairs for the lightpaths in it. There are two cases:

- *Case 1:* Fault tolerance is *not* required, or even if required, there is only *one single WDM path* between IP adjacency end nodes, or even if more than one, only one is within

the reach for at least one transponder type. In this case, the WDM path associated to the adjacency is the shortest one in optical length.

- *Case 2:* Fault tolerance is required and there are more than one different WDM paths (not necessarily link disjoint) between them within the reach for at least one transponder type. In this case, two WDM paths are assigned to the IP adjacency: the shortest ones in km, which are maximally link disjoint. This means that a valid WDM path pair is preferred if both paths have fewer WDM links in common, and then a lower sum of optical path lengths is preferred.

After that, (8) we compute the *minimum capacity* needed to be installed in the lightpaths in *each* WDM path. This is computed as follows:

- If only one WDM path exists, the capacity required is the worst-case IP traffic to be carried by the adjacency. In this case, the network will not be tolerant to the failure of the WDM links in the single WDM path.
- If two WDM paths exist, the capacity required in each WDM path is computed as the maximum between: (i) the non-failure state traffic, (ii) half of the worst case traffic in the different MCEN-BB failure states (if this is required). Note that (i) corresponds to the traffic in a WDM path, when the other WDM path is failed, and (ii) corresponds to the case when an MCEN-BB fails. Also note that in any case, the network will not be fault tolerant to the WDM links that are common to both paths, when they are not fully WDM link disjoint.

Once we compute the minimum per-WDM path capacity needed, (9) the algorithm computes for each IP adjacency the best transponder type choice to be used in all the lightpaths realizing it. Recall that because of the limitations of the hash-based load balancing of IP traffic in the LAGs, all the transponders have to be of the same line rate. Still, the final choice can be made in different forms, e.g. minimizing the total cost, or minimizing the spectral occupation. We minimize the cost in our tests.

After the transponder types have been chosen, (10) the number of lightpaths required in each WDM path is computed from the per-path minimum capacity needs, and the transponder line rate. Then, the lightpaths spectrum is allocated to each lightpath in the WDM paths, using the first fit scheme. For this: (i) if the WDM path only traverses ROADMs, the spectrum is allocated in the traversed WDM links, (ii) otherwise, the spectrum is allocated in the WDM links, and in those other fibers where the spectrum is occupied because of the D&W propagation.

All the lightpaths are bidirectional, composed of two unidirectional lightpaths in opposite routes, a common choice that simplifies network operation. In addition, the two opposite lightpaths are assigned the same wavelength. Aside of a simpler network operation, this can lead to a more cost-effective transponder hardware when coherent technologies are used, since the transmission laser can also feed the reception circuit, so two different lasers are not needed.

During the sequential lightpath creation process, it may happen that the optical spectrum in the WDM links becomes exhausted, and no spectrum allocation is possible. In these cases, the algorithm does not stop. Alternatively, we preferred to devise a *WDM plant expansion process*, which permits us to obtain

TABLE VI
TRANSPONDERS INFORMATION [36]

| Name | RATE [Gb/s] | Optical reach [Km] | Spectral width | Cost | Power consumption |
|------|----------------|-----------------------|-------------------|------|----------------------|
| TpA | 25 | 100 | 50 GHz | 2.4 | 120 W |
| TpB | 100 | 200 | 100 GHz | 5 | 160 W |

valuable information on how the long-term network will need to be upgraded. The WDM plant expansion works as follows: (i) the fibers in the congested WDM path are organized in decreasing order on the amount of occupied spectrum, (ii) a parallel fiber is added between the nodes of the first congested fiber in the list, (iii) the first-fit allocation is tried again, (iv) if not succeeded, the process is repeated with the next congested fiber in the list.

At the end of the algorithm, (12) it may occur that some fibers have been created, that are actually not used. This is evaluated, and unused newly created fibers are removed.

The algorithm has a polynomial complexity. Its running time is dominated by the RSA loop, which runs once for each IP adjacency (N^2 in the worst case, where N is the number of nodes). Inside the RSA loops, the running time is dominated in large networks by the link-disjoint shortest path calculations, which can be implemented with a complexity $O(E+N \log N)$, being E the number of fibers.

VI. SIMULATION SET UP AND NUMERICAL RESULTS

This section collects and analyzes the results of the techno-economic study aimed at evaluating the cost vs. performance trade-offs related to the two technological choices exposed: the use of filterless technologies in degree 1 and degree 2 optical nodes, and the benefits of the agile control plane. Relevant for the filterless technological choice, we conducted a series of simulations that explored candidates for filterless-based nodes up to degree 3 (results not reported here). We observed a high number of lasing loop occurrences that compromised the entire network performance (see section IV.A). Additionally, let us recall that the values in parentheses in Table I (node column) are the number of nodes with node degree 1 or 2, hence a predominant proportion for candidates to be filterless, thus with a significant economic impact.

In all the tests, we consider that MCEN-MCEN lightpaths use a 100 Gb/s coherent transponder, while the rest make use of a 25 Gb/s transponder, with the characteristics shown in Table VI. The optical reach is stated as a maximum reach, a simplification considered sufficient for the macroscopic view pursued, and targeting coherent 100 Gb/s transponders and innovative IM-DD 25 Gb/s transponders with integrated multi stage optical dispersion compensators for high chromatic dispersion tolerance in uncompensated optical networks ([41] and references therein). The cost model and power consumption estimated will be included in deliverable D2.4 of the METRO-HAUL project [42].

A. Simulation Framework

The capacity planning algorithm described in Section V, and the related scripts for running the tests have been implemented in Net2Plan [2]. The algorithms are built on top of the NIW

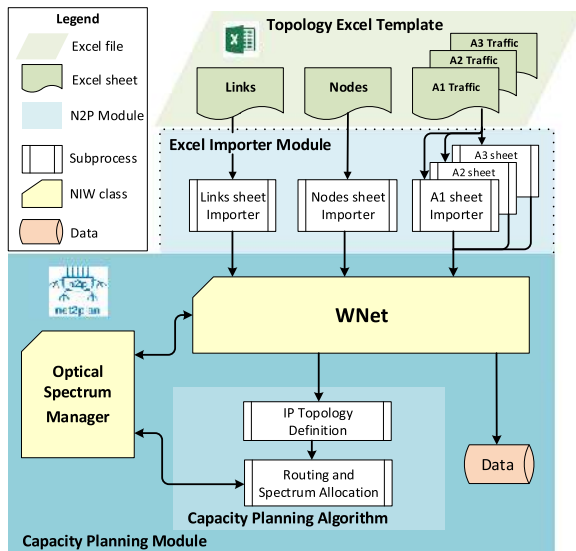


Fig. 9. Overview of the design of the techno-economic study algorithm.

TABLE VII
TOTAL NUMBER OF TRANSPONDERS FOR LONG-TERM TRAFFIC

| Topology | Planning | Tp. 25G | Tp. 100G | Total | Cost | Savings |
|----------|----------|---------|----------|-------|------|---------|
| Dense | Static | 100 | 204 | 304 | 1260 | |
| Urban | Dynamic | 96 | 188 | 284 | 1170 | -7.1% |
| Reg. | Static | 758 | 150 | 908 | 2569 | |
| Small | Dynamic | 664 | 130 | 794 | 2243 | -12.7% |
| Reg. | Static | 1702 | 238 | 1940 | 5275 | |
| Normal | Dynamic | 1533 | 204 | 1737 | 4699 | -10.9% |

library (NFV over IP over WDM) [28], developed within the METRO-HAUL project, which provides high level abstractions that facilitates and speeds-up the algorithm development.

The code of the algorithms and scripts is available in the METRO-HAUL repository under request [33]. This includes the import functions that convert the Excel sheets containing the scenarios under test, into the network model, and instance of the NIW *WNet* class (see Fig. 9). Then, Net2Plan regular graphical user interface can be used to run the developed capacity planning algorithm (Capacity Planning Module), and visualize and analyze the results. The Optical Spectrum Manager in the NIW library implements higher level abstractions for solving the routing and spectrum assignment in hybrid WDM networks with ROADMs and filterless switching nodes. Finally, while some of the data related to the reference scenarios is not freely available because of confidentiality reasons, the user can find in the repository alternative Excel files containing other realistic scenarios.

B. Assessment of the Benefits of an Agile Control Plane

This section evaluates the CAPEX and energy consumption benefits of having an agile control plane, enabling an on-demand allocation of resources as described in Section IV.

Table VII contains the results corresponding to the number of transponders needed in the three network topologies, comparing

TABLE VIII
TOTAL TRAFFIC SUPPORTED BY THE NODES FOR LONG-TERM TRAFFIC

| Topology | Planning | A1 traf. [Gb/s] | A2 traf. [Gb/s] | A3 traf. [Gb/s] | Total | Savings |
|----------|----------|-----------------|-----------------|-----------------|-------|---------|
| Dense | Static | 3472 | 2052 | 6572 | 12096 | |
| Urban | Dynamic | 3112 | 1839 | 5893 | 10844 | -10.4% |
| Reg. | Static | 3853 | 2277 | 7297 | 13427 | |
| Small | Dynamic | 3359 | 1985 | 6321 | 11665 | -13.1% |
| Reg. | Static | 8977 | 5293 | 1696 | 15966 | |
| Normal | Dynamic | 7817 | 4619 | 1480 | 13916 | -12.8% |

the static and dynamic planning cases. Recall that the dynamic planning is enabled by an agile control plane (see Section IV).

As can be seen, the savings in the number of transponders needed is significant, resulting in an overall cost reduction in CAPEX in the order of 10%, this number being topology dependent. These amounts correspond to the long-term traffic scenario. The total cost numbers have been obtained assuming the corresponding values of Table VI for each transponder type. Analogous although slightly inferior saving percentages have been observed in scenarios with lower traffic.

Note that according to the behavior of the capacity algorithm, the transponder requirements are unchanged when filterless topologies are used. The impact of filterless waste spectrum is evaluated later, with its effect in spectral efficiency and potential extra WDM plant expansion requirements.

The CAPEX savings of the agile control plane, in terms of IT infrastructure requirements has been also evaluated. The IT resources to install in a node are considered proportional to the total amount of traffic (e.g. in Gb/s) that is processed by each node, considering all the VNFs in it. Table VIII shows these results for the long-term traffic case, also giving separated numbers for the VNFs running the servers of A2 traffic, the UPFs 1 and 2, and the cache systems in the A3 traffic. In the static case, the NFs are dimensioned for the worst-case traffic, while in the dynamic case each node allocates IT resources on demand. As shown in Table VIII, CAPEX savings obtained are also in the order of 10% to 13%. Similar percentages have been found in short and medium term traffic scenarios.

In this paper, we are also interested in assessing the benefits that an agile control plane can bring in terms of energy consumption. The savings evaluated refer to two sources.

- *Energy savings when unused transponders in a node are switched off.* We estimate these savings as being proportional to the average time that transponders can be switched off along the day.
- *Energy savings when unused IT resources are deallocated.* This assumes that optimization procedures can be applied in each node data center, that switches off server blades or full racks, during underload conditions. In this paper, we estimate that the energy consumption is proportional to the amount of active IT resources in the node. This is just an approximation: the final energy savings depend on the chances to pack the running instances in the minimum possible number of machines, while still satisfying processing capacity requirements, so the emptied servers can be switched off.

TABLE IX
AVERAGE NUMBER OF ACTIVE TRANSPONDERS PER TYPE AND NODE FOR LONG-TERM TRAFFIC

| Topology | Planning | Tp. 25G / Gp. 100G / node | | Tp. energy cons. /node | Savings |
|-------------|----------|---------------------------|------|------------------------|---------|
| Dense | Static | 2.78 | 5.67 | 1241 W | |
| | Dynamic | 2.11 | 3.78 | 858W | 30.9 % |
| Urban | Static | 11.58 | 2.88 | 1850 W | |
| | Dynamic | 9.50 | 1.87 | 1439 W | 22.2 % |
| Reg. Normal | Static | 16.69 | 2.33 | 2375 W | |
| | Dynamic | 11.10 | 1.53 | 1577 | 33.6 % |

TABLE X
AVERAGE VNF TRAFFIC PER NODE

| Topology | Planning | VNF traffic [Gb/s] | Savings |
|-------------|----------|--------------------|---------|
| Dense Urban | Static | 336 | |
| | Dynamic | 204 | 39.2 % |
| Reg. Small | Static | 258 | |
| | Dynamic | 161 | 37.6 % |
| Reg. Normal | Static | 306 | |
| | Dynamic | 190 | 37.7 % |

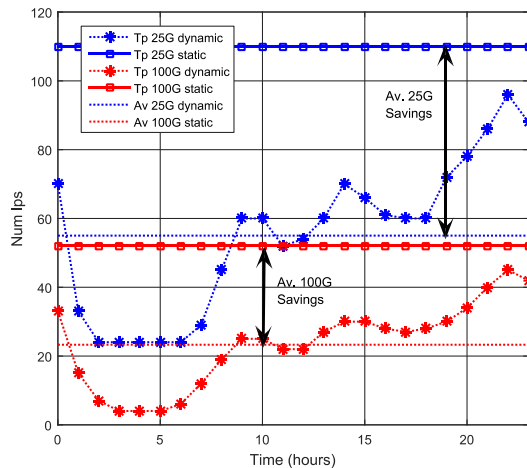


Fig. 10. Number of lightpaths used per type in a high-loaded MCEN node.

Table IX summarizes the estimated transponder energy consumption savings in the dynamic case, for the three topologies, in the long-term traffic scenario. Aggregated savings (considering a similar consumption for all transponders) are between the 22% and the 34%.

Similarly, Table X showcases the relative computational energy savings in the nodes. In this case, the dynamic approach offers up to 39% lower IT energy consumption. Similar results are obtained in the other traffic scenarios.

To further illustrate this effect, Fig. 10 shows a typical daily profile in a single MCEN node, respect to the number of active transponders of each type in the static (constant) and dynamic planning case. In its turn, Fig. 11 shows a sampled daily profile of used IT resources in a high-loaded MCEN node, with the contributions of the different traffic.

Note that the reported OPEX savings in terms of energy consumption evidence the suitability of agile control-plane solutions and their applicability in both network resources (i.e.

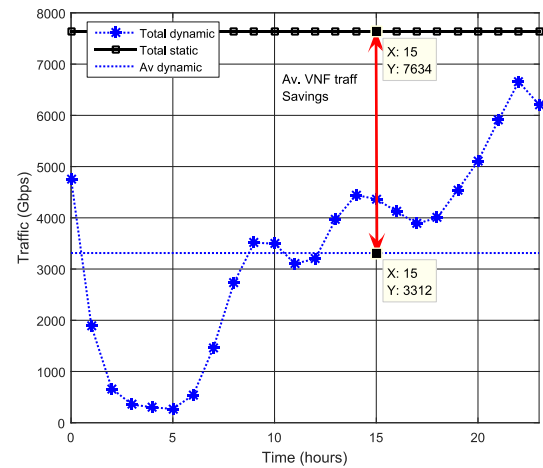


Fig. 11. Total VNF traffic in Gb/s in a high-loaded MCEN node.

TABLE XI
AVERAGE FIBER SPECTRUM OCCUPATION IN THZ FOR LONG-TERM TRAFFIC

| Topology | Planning | ROADM | D&W filterless | Filterless waste |
|-------------|----------|-------|----------------|------------------|
| Dense Urban | Static | 0.75 | 0.76 | 1.64% |
| | Dynamic | 0.69 | 0.71 | 3.51% |
| Reg. Small | Static | 0.91 | 1.06 | 14.12% |
| | Dynamic | 0.81 | 0.94 | 13.33% |
| Reg. Normal | Static | 1.21 | 1.23 | 1.02% |
| | Dynamic | 0.99 | 1.01 | 2.47% |

transponders) and IT resources. Consequently, dynamic approaches as the ones reported in [25] and [26] are suitable technologies for achieving the savings here reported. In this regard, [26] is an initiative within METRO-HAUL pursuing advanced control-plane mechanisms encompassing in a synergistic manner both network and IT resources.

C. Assessment of the Filterless Spectrum Waste Impact

This section evaluates the spectrum efficiency loss caused by the use of drop and waste architectures in the degree 1 and 2 AMENs. For this, we first introduce the concept of spectrum fragmentation [43], intensely studied in WDM networks. This refers to the inefficiencies caused by unoccupied gaps in the spectrum, that cannot be assigned to new lightpaths since then the spectrum continuity constraint would not be met. It is well known that the intensity of such fragmentation depends on the WDM topology, and worsens when multiple transponders can be used, with different spectral widths.

The first question we want to address is if the filterless operation can have an impact i) on the amount of occupied spectrum (summing the occupied and wasted spectrum in the fibers), ii) in the fragmentation efficiency, defined as the fraction between the *used* or *wasted* spectrum in the fibers, divided by the highest frequency occupied (or wasted) in the fiber. Note that the fragmentation efficiency is one when no spectral gaps are created, as the ones shown in Fig. 12.

Table XI displays the average fiber spectrum occupation values in THz, counting also the wasted spectrum in the filterless case, for the long-term traffic case, and both the static and

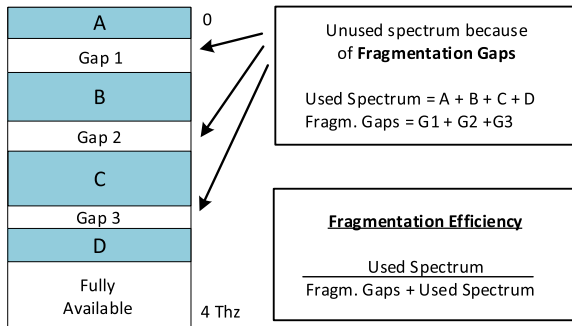


Fig. 12. Fragmentation efficiency concept explanation.

TABLE XII
AVERAGE FRAGMENTATION EFFICIENCY FOR LONG-TERM TRAFFIC

| Topology | Planning | ROADM | D&W filterless | Filterless loss |
|-------------------|----------------|-------|----------------|-----------------|
| <i>Dense</i> | Static | 0.32 | 0.33 | 3.03% |
| <i>Urban</i> | Dynamic | 0.31 | 0.31 | 0.00% |
| <i>Reg. Small</i> | Static | 0.59 | 0.62 | 4.84% |
| | Dynamic | 0.57 | 0.58 | 1.72% |
| <i>Reg.</i> | Static | 0.57 | 0.53 | -7.55% |
| <i>Normal</i> | Dynamic | 0.42 | 0.46 | 8.70% |

TABLE XIII
FIBER PLANT EXTENSION IN EXTRA FIBERS FOR LONG-TERM TRAFFIC

| Topology | Planning | ROADM | D&W filterless | Plant expansion penalties |
|--------------------|----------------|-------|----------------|---------------------------|
| <i>Dense Urban</i> | Static | 2 | 2 | 0 % |
| | Dynamic | 2 | 2 | 0 % |
| <i>Reg. Small</i> | Static | 2 | 2 | 0 % |
| | Dynamic | 0 | 0 | 0 % |
| <i>Reg. Normal</i> | Static | 14 | 16 | 12.5 % |
| | Dynamic | 8 | 8 | 0 % |

dynamic planning cases. Results show that the wasted spectrum is relatively small, between 1% and 15% of the occupied spectrum. In its turn, Table XII collects the average fragmentation efficiency values. We observe that this efficiency is relatively low, from 30% to 60% in different topologies. This is a sign that fragmentation itself has a significant impact in metro networks. However, it is interesting to observe that there is no significant extra penalty in spectrum efficiency caused by the filterless nodes. These conclusions can be drawn also from the results in the other lower traffic scenarios, not shown.

To assess the potential penalty in terms of CAPEX that the performance loss associated to drop-and-waste nodes can bring, we study the WDM capacity expansion required in each case. That is, the number of new parallel fiber links that had to be created to cope with the traffic demand. For this, Table XIII collects the results in the long-term traffic scenario, for the three WDM topologies, and both the static and dynamic planning scenarios. Interestingly, the number of extra fibers required is *the same* in all the cases, when the network is fully equipped with regular ROADMs vs. when some nodes are filterless, with one single exception when an extra bidirectional fiber link is needed in the Reg. Normal topology for the static planning case.

This is an interesting result, in line with the limited spectrum occupation and efficiency penalties shown in Tables XI and XII. Actually, results in Table XIII now show that the utilization of cost-effective filterless nodes in the degree 1 and 2 AMEN, have zero or very limited CAPEX penalties in terms of higher WDM plant expansion requisites.

The impact in terms of CAPEX and energy consumption savings that can be obtained from replacing degree 1 and 2 ROADMs by filterless switches built with passive splitters and couplers, originates from their negligible cost and power consumption. Precise numbers depend on the particular ROADM architecture to be replaced. As a hint, according to METRO-HAUL cost model [36], the per-degree cost of a WSS based ROADM is in the order of several thousand dollars, and has an associated power consumption in the order of 50 Watts, filterless switching fabrics have a cost around 100\$, and zero power consumption (but, if any, associated to shelf control).

VII. CONCLUSION

Analyzing the economic implications of the optical metro network deployment decisions is essential to foster its sustainability. In this work we presented a techno-economic effort to evaluate the cost-performance trade-offs of two relevant technological options: i) the installation of an agile control plane in the metro, capable of on-demand allocation of lightpaths and virtualized functions, and ii) the utilization of cost-effective filterless nodes in degree 1 and 2 nodes, that make a large fraction of the total nodes in the optical metro. To accomplish these targets, a complete evaluation scenario was constructed to simulate short-, medium-, and long-term traffic environments, with realistic daily fluctuation patterns, for three reference topologies under the umbrella of the METRO-HAUL project. Benchmark scenarios were carefully created to match the expected evolution of 5G traffic in the metro, and to observe their effect in realistic and close-to-real reference networks.

Our results show CAPEX benefits of an agile control plane, thanks to its capability to allocate IT and network resources on demand, in the order of 10% to 13%, better as traffic grows. Energy savings in the transponders can be in the order of 20–30%, while consumption savings in the IT resources can be in the range of 35%–40%. These numbers suggest that control plane agility is a future-proof and net saving option to consider by carriers.

The utilization of filterless nodes in degree 1 and 2 nodes has shown to be a sweet spot in the reference scenarios. The extra occupation and fragmentation caused by the wasted spectrum is small, and its potential penalty in extra WDM link requirements is very limited, if any. Thus, results validate their application in the metro to degree 1 and 2 nodes, which make more than the 50% of the nodes in the regional topologies in the reference scenarios. Finally, this work can be considered a baseline approach in which two prominent technological alternatives are synergistically explored in the pursue of economic benefits. Future works can leverage the benchmark and methodologies presented to address the rolling out of data-center functions in the central offices, for different contexts. For instance, in a

conservative scenario, the deployment of DC functions may be prevented in tiny AMEN nodes due to its economical impact, or space and power supply constraints. Alternatively, more aggressive traffic predictions with a dominance of 5G low-latency applications (e.g. driverless cars) would add constraints to DC localization that foster the spreading of computation resources in the AMENs, closer to the users, and thus altering the view in this study.

REFERENCES

- [1] METRO-HAUL Project. European Commission Horizon, 2020. [Online]. Available: <https://metro-haul.eu/>. Accessed: Nov. 2019.
- [2] Net2plan – The open-source Network Planner. [Online]. Available: www.net2plan.com. Accessed: Oct. 2019.
- [3] F. Idzikowski *et al.*, “TREND in energy-aware adaptive routing solutions,” *IEEE Commun. Mag.*, vol. 51, no. 11, pp. 94–104, Nov. 2013.
- [4] A. Fumagalli, and L. Valcarenghi, “IP restoration vs. WDM protection: Is there an optimal choice?” *IEEE Netw.*, vol. 14, no. 6, pp. 34–41, Dec. 2000.
- [5] P. Papanikolaou, K. Christodouloupoulos, and E. Varvarigos, “Joint multi-layer survivability techniques for IP-over-elastic-optical-networks,” *IEEE J. Opt. Commun. Netw.*, vol. 9, no. 1, pp. A85–A98, Jan. 2017.
- [6] R. M. Morais, J. Pedro, and A. N. Pinto, “Techno-economic analysis of fixed and flexible node architectures in multiperiod scenarios,” *IEEE J. Opt. Commun. Netw.*, vol. 7, no. 12, pp. B109–B121, Dec. 2015.
- [7] A. Eira, M. Quagliotti, and J. Pedro, “Impact of client-and line-side flexibility in the lifecycle of next-generation transport networks,” *IEEE J. Opt. Commun. Netw.*, vol. 8, no. 7, pp. A101–A115, Jul. 2016.
- [8] A. Mayoral, V. López, O. Gerstel, E. Palkopoulou, O. González de Dios, and J. P. Fernández-Palacios, “Minimizing resource protection in IP over WDM networks: Multi-layer shared backup router,” *IEEE J. Opt. Commun. Netw.*, vol. 7, no. 3, pp. A440–A446, Mar. 2015.
- [9] V. Gkamas, K. Christodouloupoulos, and E. Varvarigos, “A joint multi-layer planning algorithm for IP over flexible optical networks,” *IEEE J. Lightw. Technol.*, vol. 33, no. 14, pp. 2965–2977, Jul. 2015.
- [10] P. S. Khodashenas *et al.*, “Benefit evaluation of all-optical subchannel add-drop in flexible optical networks,” *IEEE Photon. J.*, vol. 8, no. 2, Apr. 2016, Art. no. 0601708.
- [11] C. A. S. Diniz *et al.*, “Network cost savings enabled by probabilistic shaping in DP-16QAM 200-Gb/s systems,” in *Proc. Opt. Fiber Commun. Conf.*, Anaheim, CA, USA, Mar. 2016, p. Tu3F.7.
- [12] J. Pedro and N. Costa, “Optimized hybrid raman/EDFA amplifier placement for DWDM mesh networks,” *IEEE J. Lightw. Technol.*, vol. 36, no. 9, pp. 1552–1561, May 2018.
- [13] “5G infrastructure public private partnership (5G PPP) key performance indicators (KPIs),” [Online]. Available: <https://5g-ppp.eu/kpis>. Accessed: Nov. 2019.
- [14] T. O. Olwal, K. Djouani, and A. M. Kurien, “A survey of resource management toward 5G radio access networks,” *IEEE Commun. Surv. Tut.*, vol. 18, no. 3, pp. 1656–1686, 2016.
- [15] B. Gangopadhyay, J. Pedro, and S. Spaelter, “5G-Ready multi-failure resilient and cost-effective transport networks,” *IEEE J. Lightw. Technol.*, vol. 37, no. 16, pp. 4062–4072, Aug. 2019.
- [16] M. Jaber, M. A. Imran, R. Tafazolli, and A. Tukmanov, “5G backhaul challenges and emerging research directions: A survey,” *IEEE Access*, vol. 4, pp. 1743–1766, Apr. 2016.
- [17] A. Basta, A. Blenk, K. Hoffmann, H. J. Morper, M. Hoffmann, and W. Kellerer, “Towards a cost optimal design for a 5G mobile core network based on SDN and NFV,” *IEEE Trans. Netw. Service Manage.*, vol. 14, no. 4, pp. 1061–1075, Dec. 2017.
- [18] M. Savi, M. Tornatore, and G. Verticale, “Impact of processing costs on service chain placement in network functions virtualization,” in *Proc. IEEE Conf. Netw. Function Virtualization Soft. Defined Netw.*, Nov. 2015, pp. 191–197.
- [19] L. Askari, A. Hmaity, F. Musumeci, and M. Tornatore, “Virtual-network-function placement for dynamic service chaining in metro-area networks,” in *Proc. Opt. Netw. Des. Model.*, Dublin, Ireland, May 2018, pp. 136–141.
- [20] A. Tzanakaki, and M. O’Mahony, “Analysis of filterless wavelength converters employing cross-gain modulation in semiconductor optical amplifiers,” in *Proc. Conf. Lasers Electro-Opt.*, Baltimore, MD, USA, May 1999, pp. 433–434.
- [21] A. Muhammad, M. Furdek, G. Zervas, and L. Wosinska, “Filterless networks based on optical white boxes and SDM,” in *Proc. Eur. Conf. Opt. Commun.*, Dusseldorf, Germany, Sep. 2016, pp. 1–3.
- [22] J. Pedreno-Manresa, J. Izquierdo-Zaragoza, F. Cugini and P. Pavon-Marino, “On the benefits of elastic spectrum management in multi-hour filterless metro networks,” in *Proc. Opt. Netw. Des. Model.*, Dublin, Ireland, May 2018, pp. 184–189.
- [23] R. Aparicio-Pardo, N. Skorin-Kapov, P. Pavon-Marino, and B. Garcia-Manrubia, “(Non)-reconfigurable virtual topology design under multi-hour traffic in optical networks,” *IEEE/ACM Trans. Netw.*, vol. 20, no. 5, pp. 1567–1580, Oct. 2012.
- [24] R. Aparicio-Pardo, B. Garcia-Manrubia, P. Pavon-Marino, N. Skorin-Kapov, and M. Furdek, “Balancing CapEx reduction and network stability with stable routing-virtual topology capacity adjustment (SR-VTCA),” *Elsevier Opt. Switching Netw.*, vol. 10, no. 4, pp. 343–353, Nov. 2013.
- [25] R. Martínez *et al.*, “Integrated SDN/NFV orchestration for the dynamic deployment of mobile virtual backhaul networks over a multilayer (packet/optical) aggregation infrastructure,” *IEEE J. Opt. Commun. Netw.*, vol. 9, no. 2, pp. A135–A142, Feb. 2017.
- [26] R. Casellas, R. Martínez, R. Vilalta, and R. Muñoz, “Control, management, and orchestration of optical networks: Evolution, trends, and challenges,” *IEEE J. Lightw. Technol.*, vol. 36, no. 7, pp. 1390–1402, Apr. 2018.
- [27] J. L. Romero-Gázquez, M. V. Bueno-Delgado, F. J. Moreno-Muro, and P. Pavón-Mariño, “Net2plan-GIS: An open-source Net2Plan extension integrating GIS data for 5G network planning,” in *Proc. Int. Conf. Transp. Opt. Netw.*, Bucharest, Romania, Jul. 2018, pp. 1–4.
- [28] J. L. Romero-Gázquez, M. Garrich, F. J. Moreno-Muro, M. V. Bueno-Delgado, and P. Pavón-Mariño, “NIW: A Net2Plan-based library for NFV over IP over WDM networks,” in *Proc. Int. Conf. on Transp. Opt. Netw.*, Angers, France, Jul. 2019, pp. 1–4.
- [29] R. Rumipamba, F. J. Moreno-Muro, J. Perelló, P. Pavón-Mariño, and S. Spadaro, “Space continuity constraint in dynamic flex-grid/SDM optical core networks: An evaluation with spatial and spectral super-channels,” *Elsevier Comput. Commun.*, vol. 126, pp. 38–49, Aug. 2018.
- [30] E. Riccardi, P. Gunning, O. González-de-Dios, M. Quagliotti, V. López, and A. Lord, “An operator view on the introduction of white boxes into optical networks,” *IEEE J. Lightw. Technol.*, vol. 36, no. 15, pp. 3062–3072, Aug. 2018.
- [31] F. J. Moreno-Muro, C. San-Nicolás, M. Garrich, P. Pavón, O. González de Dios, and R. Lopez Da Silva, “Latency-aware optimization of service chain allocation with joint VNF instantiation and SDN metro network control,” in *Proc. Eur. Conf. Opt. Commun.*, Rome, Italy, Sep. 2018, pp. 1–3.
- [32] M. Garrich, M. Hernandez-Bastida, C. San-Nicolás, F. J. Moreno-Muro, and P. Pavón-Mariño, “The Net2Plan-openstack project: IT resource manager for metropolitan SDN/NFV ecosystems,” in *Proc. Opt. Fiber Conf. (OFC)*, San Diego, CA, USA, Mar. 2019, p. M3Z.16.
- [33] GitLab METRO-HAUL repository. [Online]. Available: <https://gitlab.com/metro-haul>. Accessed: Nov. 2019.
- [34] M. Garrich *et al.*, “Experimental demonstration of function programmable add/drop architecture for ROADMs,” *J. Opt. Commun. Netw.* vol. 7, no. 2, pp. A335–A343, 2015.
- [35] Specification 3GPP TS 23.501 V15.2.0 (2017-12) System Architecture for the 5G System.
- [36] Metro-Haul Project - Deliverable 2.3, “Network architecture definition, design methods and performance evaluation,” Oct. 15, 2019. [Online]. Available: <https://zenodo.org/record/3496939>. Accessed on: Nov. 2019.
- [37] *IEEE Link Aggregation Task Force*. IEEE P802.3ad, Mar. 2000.
- [38] P. Pavon *et al.*, “Hands-on demonstration of open-source filterless-aware offline planning and analysis tool for WDM networks,” in *Proc. Opt. Fiber Commun. Conf.*, San Diego, CA, USA, 2020, Paper M3Z.7.
- [39] Autoscaling groups in OpenStack Heat. [Online]. Available: <https://wiki.openstack.org/wiki/Heat/AutoScaling>. Accessed: Nov. 2019.
- [40] M. Garrich, F. J. Moreno-Muro, M. V. Bueno-Delgado, and P. Pavón-Mariño, “Open-source network optimization software in the open SDN/NFV transport ecosystem,” *IEEE J. Lightw. Technol.*, vol. 37, no. 1, pp. 75–88, Jan. 2019.
- [41] METRO-HAUL Project-Deliverable 3.2, “First validation of the METRO-HAUL node architecture and optical solutions,” Oct. 15, 2019. [Online]. Available: <https://zenodo.org/record/3497044>. Accessed: Nov. 2019.
- [42] METRO-HAUL Project - Deliverable 2.4. Apr. 2020. [Online]. Available: <https://zenodo.org/communities/metro-haul/>. Accessed: Nov. 2019.
- [43] Y. Kwon, D. K. Park, and H. Rhee, “Spectrum fragmentation: Causes, measures and applications,” *Elsevier Telecommun. Policy*, vol. 41, no. 5–6, pp. 447–459, Jun. 2017.